Electronic Characteristics and Charge Transport Mechanisms for Large Area Aromatic Molecular Junctions

Adam Johan Bergren[1*], Richard L. McCreery[1,2], Stanislav R. Stoyanov,[1] Sergey Gusarov,[1] and Andriy Kovalenko[1,3]

[1]National Institute for Nanotechnology, National Research Council Canada, Edmonton, Alberta, Canada

[2]Department of Chemistry, University of Alberta, Edmonton, Alberta, Canada

[3]Department of Mechanical Engineering, University of Alberta, Edmonton, Alberta, Canada

Email: Corresponding author: Adam.Bergren@nrc.ca (AJB)

Supporting Information to "Electronic Characteristics and Charge Transport Mechanisms for Large Area Aromatic Molecular Junctions"

This document contains additional supporting data, discussion, and derivations of equations used to analyze data and calculate *J-V* curves. Specifically:

1. Procedure for lifetime testing (Figure 2 in main text)
2. Effect of aging of finished junctions
3. *J-V* curves of Figure 3 on linear scale
4. Dependence of β on bias
5. Arrhenius slopes for five molecules and several thicknesses
6. Capacitance and dielectric constant determination
7. Molecular orbitals for azobenzene dimer and tetramer and calculated barriers for aromatic systems

1. Comment regarding Figure 2: The high speed data acquisition system utilizes a National Instruments NI 5421 arbitrary function generator rated at 100 Ms/s (up to 43 MHz) and a 2-channel NI 5124 high speed digitizer (200 Ms/s) for data acquisition. The recorded results correct for voltage losses in the PPF by directly measuring the voltage at a probe placed at a position equidistant from the junction relative to the drive lead using one channel of the digitizer. The current is recorded by measuring the voltage drop between the top contact and a measurement resistor using the second channel of the digitizer. This does not compensate for *iR* drip in the top contact (which is important when *V*, and therefore, *i* is large). Thus, the linear characteristic of *J* at voltages greater than ~0.4 V represents the series resistance of the Cu/Au lead. In all other cases reported in this paper, a four wire measurement system is used to avoid this error.

2. Figure S-1 shows an overlay of *i-V* curves for a PPF/NAB(3.3)/Cu junction within one week of fabrication (blue curve) and after aging for 271 days in air (red curve).

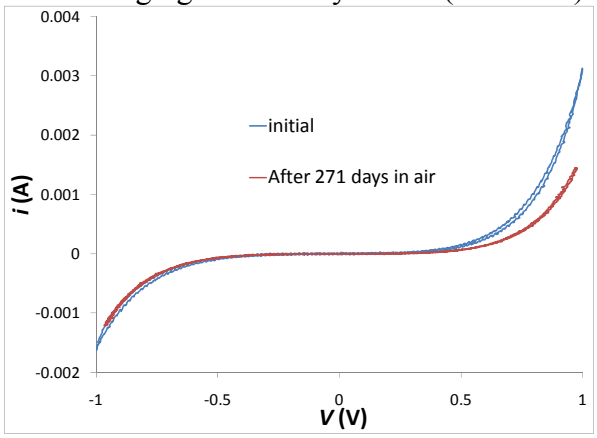

Figure S-1. Overlay of *i-V* curves for a PPF/NAB(3.3)/Cu device before and after aging in air for an extended time. Only a minimal change in current is observed, which could originate from a variety of sources.

3. Figure S-2 shows the *J*-*V* curves in Figure 3 of the main text using a linear *J* scale to clearly show the shape (in particular, linearity at low bias).

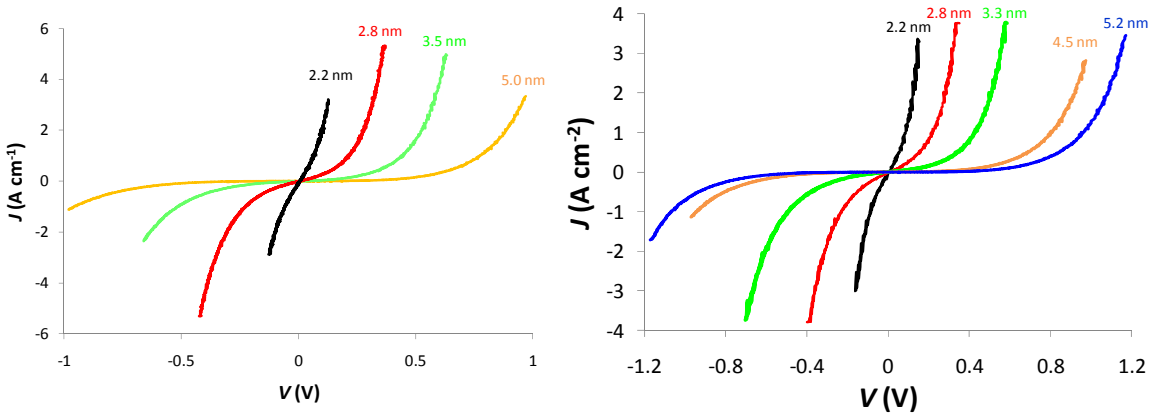

Figure S-2. Linear *J*-*V* curves for the series of AB (top) and NAB(bottom) junctions with variable thickness (see Figure 3 in main text). Junction area was 0.0017 cm^2 for NAB (bottom) and 0.0012 cm^2 for AB (top).

4. As shown in Figure S3a, β varies with bias, decreasing for greater magnitude of bias in either polarity. Wang, Lee and Reed[1] analyzed this effect to extract a zero-bias attenuation factor and an apparent barrier height, based on equations S-1 and S-2: Although their analysis assumes that the barrier height is independent of molecule length, we used their approach for comparison.

(a)

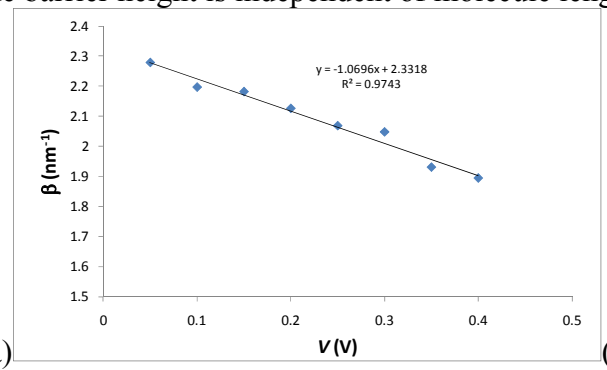

(b)

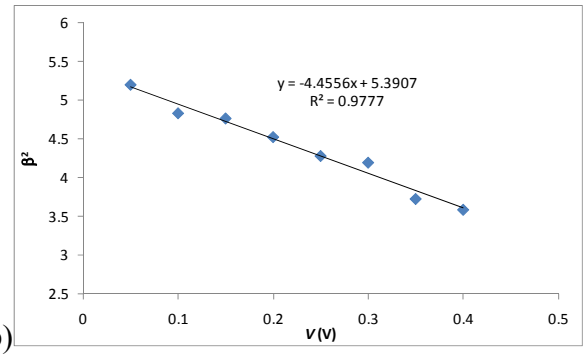

Figure S-3. Plot of β vs. *V* (a) and β^2 vs. *V* (b) for NAB junctions with 3.3, 4.5, and 5.2 nm thicknesses.

$$\beta(V) = \beta_0\left(1 - \frac{qV}{2\phi}\right)^{\frac{1}{2}} \qquad \text{(S-1)}$$

where β_0 is the extrapolated value for β at zero voltage (the bias-independent value), *q* is the elementary charge, *V* is the bias voltage, and ϕ is the tunneling barrier. This leads to

$$\beta^2 = \beta_0^2 - \beta_0^2\frac{qV}{2\phi} \qquad \text{(S-2)}$$

such that the slope and intercept of a plot of β^2 vs. *V* give values for β_0 and ϕ. Figure S-3b shows a plot of β^2 vs. *V* with the equation resulting from linear regression analysis for the data in the inset of Figure S-3b In addition, a value for α can be obtained from

$$\beta_0 = \frac{2(2m)^{\frac{1}{2}}}{\hbar}\alpha\phi^{\frac{1}{2}} \qquad \text{(S-3)}$$

where α represents a parameter that accounts for non-rectangular barrier shapes, an effective electron mass, or both. This analysis gives $\beta_0 = 2.32$ nm^{-1}, $\phi = 0.60$ eV, and $\alpha = 0.73$. If α is stated as an effective electron mass as presented in the main text, m_e becomes 0.53 m_o. Although these values are similar to those deduced from the NAB variation with thickness, we note that better correspondence between predicted and experimental *J*-*V* curves over the entire thickness and voltage range is achieved when ϕ_0 and m_e vary with molecular layer thickness.

5. Table S-1. Values for apparent activation energies obtained from linear regression analysis of Arrhenius plots.

Molecule (thickness, nm)	**5-250 K range (meV)[a]**	**260-450 K range (meV)[a]**
BP(1.4)	0.32 ± 0.11[b]	35.9 ± 1.7
FL(1.8)	0.13 ± 0.03	37.9 ± 2.1
NAB(3.3)	0.11 ± 0.04	35.6 ± 7.9
AB(3.2)	0.17 ± 0.10	102.2 ± 8.0
NAB(4.5)	0.17 (0.9 V)[c]	40 (0.25 V)
NBP(4.1)	0.020 (0.25 V)	-
NBP(4.1)	0.04 (0.5 V)	-

[a]The value of *J* used to construct the Arrhenius plots were taken at 0.2 V unless otherwise stated in parenthesis after the value.

[b]The error in the slope was determined by using the average standard deviation in the measured value of *J* for all data points in the Arrhenius plot (determined by averaging *J* over the range from 0.20 to 0.21 V, usually about 10 data points). Thus, the error in slope is estimated as σ_{avg} x (N/(N x $\Sigma x^2 - (\Sigma x)^2$)), where N is the number of data points used to construct the line, and x is the value of 1000/T for each data point[2]. Also, the standard deviation used for this analysis was based on the logarithmic error in the Arrhenius plot determined from error propagation.

[c]conductivity for this junction was too low at 0.25 V to obtain a reliable estimate of the slope. Also, the range for the low temperature region was 100-200 K and 293-400 for the high temperature region.

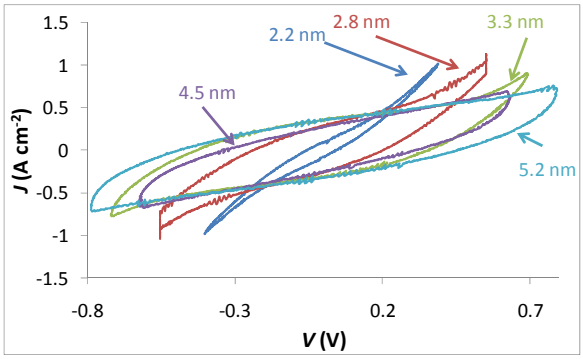

Figure S-4. *J-V* curves for a series of molecular junctions with increasing molecular layer thickness collected using a 50 kHz triangle wave for the applied voltage. The value of *J* at 0 V (the average of the absolute value of J_{0V} for each scan segment) was used to calculate the dielectric constant for the molecular layer.

6. The value of the dielectric constant (ε) can be determined from the following equation:

$$\varepsilon = \frac{J_{0V} d}{\varepsilon_0 \nu} \qquad \text{(S-4)}$$

where J_{0V} is the current density at 0 V (A cm^{-2}), d is the thickness of the molecular layer in cm, ε_0 is the permittivity of free space (8.85 x 10^{-14} F cm^{-1}), and ν is the scan rate in V s^{-1}. The values we obtain for ε using this analysis may not be fully accurate due to the possibility that the simple capacitor model we used does not fully describe the observed current in Figure S-4. However, the important issue is the change in ε with thickness, which occurs throughout the frequency range tested, and therefore is likely to be general, and not an artifact due to equivalent circuit effects or parasitic contributions to the measured current.

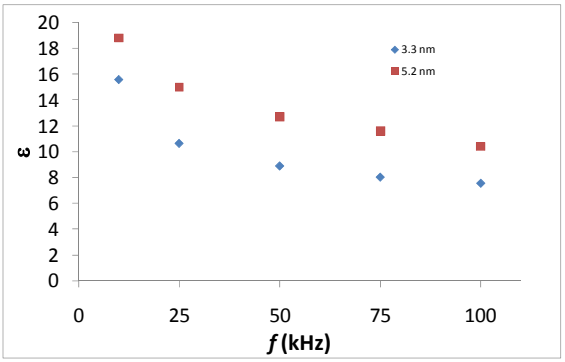

Figure S-5. Examples of the frequency dependence of ε for NAB molecular junctions.

7. Highest Occupied Molecular Orbital Visualizations for azobenzene dimer and tetramer, calculated with B3LYP-631G(d) method and calculated barriers for aromatic systems.

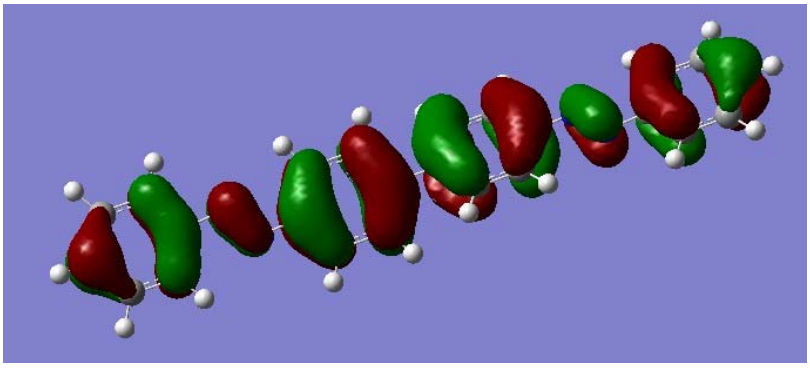

Figure S-6. Visualization of the HOMO for AB_2 molecule calculated with DFT (B3LYP/6-31G(d) basis set). The distance between the most distal H atoms is 2.2 nm, and the energy of this orbital is -6.18 eV.

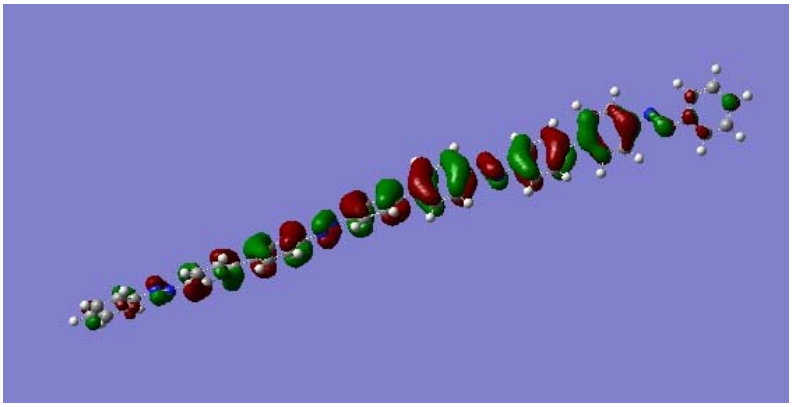

Figure S-7. Visualization of the HOMO for AB_4 molecule calculated with DFT (B3LYP/6-31G(d) basis set). The distance between the most distal H atoms is 4.3 nm, and the energy of this orbital is -5.66 eV.

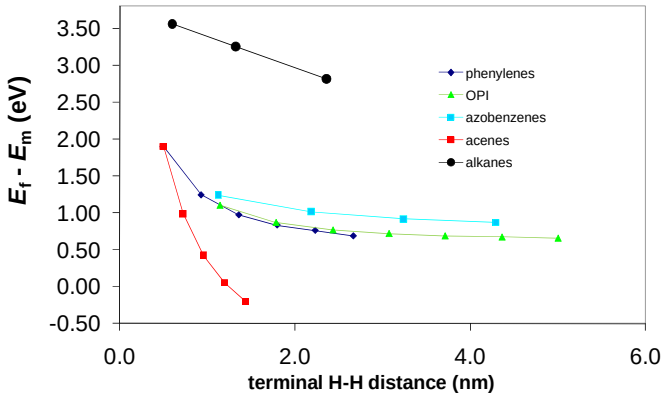

Figure S-8. DFT calculated values for the barrier height for a series of different molecules: a series of *p*-bonded phenyl rings (phenylenes, dark blue diamonds), oligophenyleneimine (OPI , green triangles), azobenzenes (light blue squares), acenes (red squares), and alkanes (black circles).

References

(1) Wang, W.; Lee, T.; Reed, M. A. *Phys. Rev. B* **2003**, *68*, 035416.
(2) Taylor, J. R. *An Introduction to Error Analysis: The Study of Uncertainties in Physical Measurements*; 2nd ed.; University Science Books: Sausalito, California, 1997.